

ACCEPTED MANUSCRIPT

This is an early electronic version of an as-received manuscript that has been accepted for publication in the Journal of the Serbian Chemical Society but has not yet been subjected to the editing process and publishing procedure applied by the JSCS Editorial Office.

Please cite this article as R. Ghibate, M. Ben Baaziz, A. Amechrouq, R. Taouil, O. Senhaji, *J. Serb. Chem. Soc.* (2024) <https://doi.org/10.2298/JSC230317037G>.

This “raw” version of the manuscript is being provided to the authors and readers for their technical service. It must be stressed that the manuscript still has to be subjected to copyediting, typesetting, English grammar and syntax corrections, professional editing and authors’ review of the galley proof before it is published in its final form. Please note that during these publishing processes, many errors may emerge which could affect the final content of the manuscript and all legal disclaimers applied according to the policies of the Journal.



J. Serb. Chem. Soc. **00(0)** 1-16 (2024)
JSCS-12322

The performance of an eco-friendly adsorbent for methylene blue removal from aqueous solution: Kinetic, isotherm, and thermodynamic approaches

RAJAE GHIBATE^{1*}, MERYEM BEN BAAZIZ², ALI AMECHROUQ³, RACHID TAOUIL⁴
and OMAR SENHAJI³

¹Laboratory of Physical Chemistry, Materials and Environment, Faculty of Sciences and Technologies, Moulay Ismail University of Meknes, Errachidia, Morocco, ²Laboratory of Materials Engineering for the Environment and Natural Resources, Faculty of Sciences and Technologies, Moulay Ismail University of Meknes, Errachidia, Morocco, ³Laboratory of Biomolecular and Macromolecular Chemistry, Moulay Ismail University of Meknes, Meknes, Morocco, and ⁴Laboratory of Mechanics, Energetics, Automation, and Sustainable Development, Faculty of Science and Technology, Moulay Ismail University of Meknes, Errachidia, Morocco

(Received 17 March 2023; revised 1 May 2023; accepted 26 March 2024)

Abstract: The current study aims to determine how well pomegranate peel can remove Methylene Blue (MB) from an aqueous solution. For this purpose, kinetic, isotherm, and thermodynamic adsorption studies were performed in a batch system. The rate of MB adsorption was rapid and reached equilibrium at about 60 minutes. The adsorption capacity reached approximately 42.71 mg g⁻¹ at the initial dye concentration of 100 mg L⁻¹. The kinetic modeling of MB adsorption was conducted using pseudo-first-order, pseudo-second-order, Elovich, and intraparticle diffusion models. The pseudo-second-order model was found to be the most adequate for fitting the kinetic data based on R², RMSE, ARE, and χ^2 values. It was also discovered that MB adsorption onto pomegranate peel is not simply rate-limited by intraparticle diffusion. The isotherm approach showed a maximum adsorption capacity of 67.78 mg g⁻¹ at 298 K using 2 g L⁻¹ of pomegranate peel. Equilibrium modeling was also conducted. The four statistical values highlighted the better fit of the Langmuir model than the Freundlich model. Additionally, the exothermic and spontaneous nature of the adsorption process was revealed by thermodynamic research. These findings demonstrate the effectiveness of pomegranate peel as an eco-friendly adsorbent for MB removal.

Keywords: adsorption; kinetic; pomegranate peel; methylene blue; isotherm, thermodynamic.

* Corresponding author. E-mail: rajae.ghibate@gmail.com
<https://doi.org/10.2298/JSC230317037G>

INTRODUCTION

Methylene blue is one of the most widely utilized synthetic dyes in various industrial sectors.¹ It is known for its promising potential in dyeing cotton, wool, and silk,² making it a common choice in the textile industry. However, the release of MB into the environment poses aesthetic issues and dramatic effects on aquatic life,³ attributed to its visibility, low biodegradability, and bioaccumulation through the food chain, posing a danger to human health. Acute exposure to MB can cause tachycardia, cyanosis, jaundice, quadriplegia, and tissue necrosis in humans.⁴ It also causes eye burns, leading to permanent injury to the eyes of humans and animals.⁵ Other adverse effects of MB, such as hypertension, acute kidney failure, and hemolytic anemia, have been reported in the literature.^{6,7} In this context, various conventional methods have been investigated to remediate water pollution caused by MB. These methods include adsorption,⁸⁻¹² classical and advanced chemical oxidation,¹³⁻¹⁷ membrane separation,^{18,19} and coagulation/flocculation,²⁰⁻²² Among these approaches, adsorption is an effective and low-cost technique to remove different pollutants from aqueous solutions,²³⁻²⁶ including MB. The significant advantages of the adsorption process include its effectiveness and economical dye removal, low sludge production, and simplicity in execution.²⁷ Additionally, utilizing agricultural waste as a biosorbent offers a low-cost and eco-friendly approach to a circular economy.²⁸ Several researchers have demonstrated the potential of various agricultural wastes for MB removal, such as sugarcane bagasse,²⁹ rice husk,⁴ date pits,³⁰ peanut hull,³¹ soursop residues,²⁹ wheat straw,³² and orange and banana peels.³³

The pomegranate is a prized fruit, valued for its unquestionable qualities that promote consumption. Global pomegranate production continues to rise owing to the high demand for the fruit and its derivatives, such as juice, syrup, and jam. However, the peel, constituting approximately 50 % of the fruit's mass,³⁴ is often discarded as waste despite its potential uses. The worldwide generation of pomegranate peel was estimated at around 1.9 million tons five years ago.³⁵ Furthermore, Morocco produces a substantial amount of pomegranate fruit, with an estimated annual production of pomegranate peel reaching 29,000 tons based on the approximately 58,000 tons of fruit harvested annually.³⁶ In this context, this research aims to enhance the performance of pomegranate peel as an eco-friendly adsorbent for removing MB from an aqueous solution. A preliminary study revealed its potential use for the adsorption of MB.³⁵ Therefore, the present work focuses on studying the kinetic, isotherm, and thermodynamic approaches to gather more information on the mechanism of MB adsorption by pomegranate peel.

EXPERIMENTAL

Adsorbate

Methylene blue, with the molecular formula $C_{16}H_{18}ClN_3S$ (Fig. 1), was supplied by Loba Chemie. It was used without further purification to prepare the stock solution (1000 mg L^{-1}). The working solutions of MB were subsequently prepared by diluting the stock solution with distilled water.

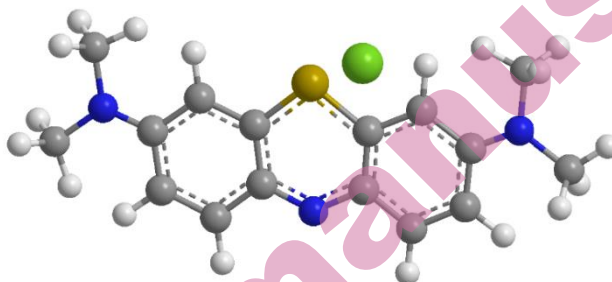


Fig. 1. Chemical structure of methylene blue dye

Biosorbent preparation

After separation from the pomegranate, the peel is cleaned with distilled water and dried in the sun for about three weeks. The fragments are ground into a powder and washed repeatedly with distilled water until a colorless solution is obtained. The powdered pomegranate peel is then dried at $60 \text{ }^\circ\text{C}$ for 48 hours before being placed in a desiccator, awaiting usage.

ATR-FTIR characterization

The surface functionalities of the produced pomegranate peel powder were identified using Attenuated Total Reflectance-Fourier Transform Infrared (ATR-FTIR) on a Themoscientific Nicolet iS10 FTIR Spectrometer. The samples were recorded in transmittance mode.

Adsorption experiments

The adsorption experiments in the present study were conducted in a batch system using the initial pH of the MB solution. For each experiment, 0.1 g of powdered pomegranate peel was added to 50 mL of the MB solution (100 mg L^{-1}) in a 100 mL Erlenmeyer flask. The suspensions were shaken at 300 rpm by an electromagnetic stirrer. The studied concentration was chosen based on the preliminary investigation assessing the effective MB concentration in textile wastewater. The adsorption kinetic approach was carried out from 0 to 300 min at room temperature. The adsorption isotherm approach was performed at 298 K for 120 min by varying the initial dye concentration from 0 to 500 mg L^{-1} . The thermodynamic approach was conducted at varying temperatures from 298 to 328 K for 120 min. At the end of each adsorption experiment, the suspensions were centrifuged at 3800 rpm for 5 min. Then, the residual concentration of MB in the supernatant was determined using a double-beam UV-Vis spectrophotometer at 665 nm. The amount of MB adsorbed per unit mass of adsorbent (q_t) was calculated using the following equation:

$$q_t = \frac{(C_0 - C_t)}{m} \cdot V \quad (1)$$

where C_0 and C_t are, respectively, the initial and time t concentrations of MB in solution, $\text{mg}\cdot\text{L}^{-1}$. V represents the MB solution volume, L, and m is the mass of the powdered pomegranate peel, g.

Kinetic study

The kinetic approach was investigated to determine the order of the adsorption reaction and the mechanism controlling the process. In this regard, four well-known models were used to study the kinetic of MB adsorption onto pomegranate peel: pseudo-first-order (PFO), pseudo-second-order (PSO), Elovich, and intraparticle diffusion (IPD), as detailed in Table I.

TABLE I. Adsorption kinetic models

Kinetic model	Non-linear	Linear		Ref.
	$\frac{dq_t}{dt} = K_2(q_e - q_t)^2$	$\frac{1}{q_t} = \frac{1}{K_2 q_e^2} + \frac{1}{q_e} t$	t/q_t vs t	38
	$\frac{dq_t}{dt}$	$q_t = \frac{1}{\beta_E} \ln(\alpha_E \beta_E) + \frac{1}{\beta_E} \ln t$	q_t vs $\ln t$	39
IPD	-	$q_t = K_{ID} t^{1/2} + c$	q_t vs $t^{1/2}$	40

where $q_e / \text{mg g}^{-1}$ and K_1 / min^{-1} represent, respectively, the amount of MB adsorbed at equilibrium and the rate constant of PFO; $K_2 / \text{g mg}^{-1} \text{min}^{-1}$ represents the rate constant of PSO; $\alpha_E / \text{mg g}^{-1} \text{min}^{-1}$ and $\beta_E / \text{g mg}^{-1}$ represent the rates constants of adsorption and desorption of Elovich, respectively; $K_{ID} / \text{mg g}^{-1} \text{min}^{-1/2}$ represents the IPD rate constant and c the constant related to the thickness of the boundary layer.

Isotherm study

The study of the adsorption isotherm is essential for quantifying and comparing the performance of pomegranate peel in MB removal. In this regard, Langmuir and Freundlich models were employed. The Langmuir isotherm model presupposes that all adsorption sites on the adsorbent are structurally homogeneous, the adsorption is confined to a monolayer, and molecules adsorbed on neighboring sites do not interact⁴¹. Accordingly, when an adsorbent reaches an equilibrium saturation point, no further adsorption occurs, indicating a finite capacity for adsorption.

$$q_e = \frac{q_{max} K_L C_e}{1 + K_L C_e} \quad (1)$$

The Langmuir equation may be expressed in its linearized form as follows:

$$\frac{C_e}{q_e} = \frac{1}{K_L q_{max}} + \frac{C_e}{q_{max}} \quad (2)$$

where $q_{max} / \text{mg g}^{-1}$ denotes the maximum adsorption capacity and $K_L / \text{L mg}^{-1}$ represents the Langmuir constant.

The Freundlich adsorption isotherm is an empirical model used to elucidate multilayer adsorption with interactions between molecules adsorbed on heterogeneous surfaces featuring non-identical sites and varied adsorption energies. This model is not restricted to the formation of monolayers of adsorbate molecules on the adsorbent⁴². Equation (4) illustrates the Freundlich isotherm model.

$$q_e = K_F C_e^{1/n} \quad (3)$$

The linearized form of the Freundlich model can be expressed as follows:

$$\ln q_e = \ln K_F + \frac{1}{n} \ln C_e \quad (4)$$

where $K_F / (\text{mg g}^{-1})(\text{L g}^{-1})^n$ is the Freundlich constant and n is the Freundlich exponent.

Analysis of models

The use of error functions is an effective way to assess the fit of a model and its underlying assumptions. This study employed four statistics: coefficient of determination (R^2), Root Mean Square Error ($RMSE$), Average Relative Error (ARE), and Chi-Square (χ^2). The optimal model should have a coefficient of determination close to one and the lowest values of $RMSE$, ARE , and χ^2 .

The $RMSE$, ARE , and χ^2 are calculated using the following expressions:

$$RMSE = \sqrt{\frac{\sum_{i=1}^N (q_{t,cal} - q_{t,exp})^2}{N}} \quad (5)$$

$$ARE = \frac{100}{N} \sum_{i=1}^N \left| \frac{q_{t,exp} - q_{t,cal}}{q_{t,exp}} \right| \quad (6)$$

$$\chi^2 = \sum_{i=1}^N \frac{(q_{t,exp} - q_{t,cal})^2}{q_{t,cal}} \quad (7)$$

where N is the number of experimental data points, $q_{t,exp} / \text{mg g}^{-1}$ is the experimental value, and $q_{t,cal} / \text{mg g}^{-1}$ is the predicted value of q_t with the investigated model.

RESULTS AND DISCUSSION

ATR-FTIR characterization

The ATR-FTIR spectrum of the studied biosorbent is illustrated in Fig. 2. The infrared spectrum of pomegranate peel exhibits bands at $3,368 \text{ cm}^{-1}$ (hydroxyl group of carboxylic acid or phenol), 2925 and 2853 cm^{-1} (C-H stretching vibrations of lignocellulosic components), 1730 cm^{-1} (C=O stretching vibration of carboxyl groups), 1615 cm^{-1} (aromatic C=C or COO^- stretching vibration of carboxylic acids), 1444 cm^{-1} (asymmetric deformation of C-H bond of methyl and methylene groups), and 1327 cm^{-1} (symmetrical deformation of C-H bond of methyl group). Other bands are attributed to the C-O vibration of primary alcohols (C-OH) of cellulose and hemicellulose.

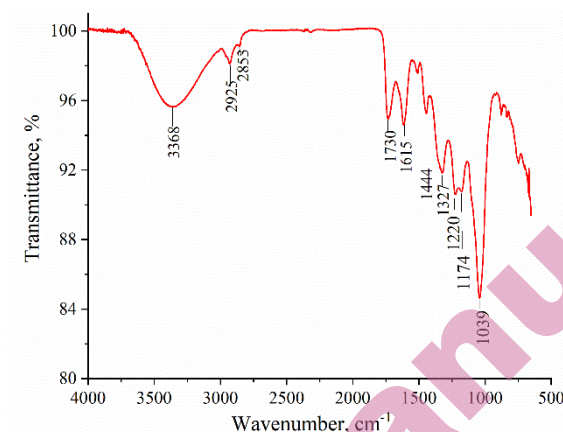


Fig. 2. ATR-FTIR spectrum of pomegranate peel powder

Adsorption kinetic

The kinetic study of MB adsorption onto pomegranate peel was conducted over a range of contact times from 5 to 300 minutes. The results depicted in Fig. 3 clearly illustrate a two-stage adsorption process. Initially, there was a rapid increase in MB adsorption, reaching 33.94 mg g^{-1} within just 10 minutes. Subsequently, the rate of MB adsorption slowed down, gradually reaching its maximum around 60 minutes, with no significant changes observed thereafter. This behavior can be attributed to numerous vacant sites on the pomegranate peel surface during the initial stage, which were rapidly occupied by MB molecules until saturation was achieved.

Additionally, to better understand the adsorption ability of the produced biosorbent, the adsorption kinetic of Rhodamine B (RhB) dye onto pomegranate peel was previously investigated. The rate of RhB adsorption was rapid, reaching equilibrium at approximately 120 minutes, with an adsorption capacity of around 30.47 mg g^{-1} .²⁷ However, it's noteworthy that this value is lower than that observed for MB adsorption, which reached 42.71 mg g^{-1} , indicating a higher affinity of pomegranate peel for MB dye.

Kinetic modeling

Four kinetic models were fitted to the obtained kinetic data: PFO, PSO, Elovich, and IPD (Fig. 4). The kinetic parameters and the associated statistical analysis of each model are presented in Table II. The suitability of the PSO model to fit the MB adsorption onto pomegranate peel can be inferred from a simple review of the preceding table. Indeed, this model presents the highest coefficient of determination ($R^2 = 1$) and the lowest values of *RMSE*, *ARE*, and χ^2 . Additionally, the fit adequacy of the PSO model for MB adsorption has been revealed by other researchers as well⁴³.

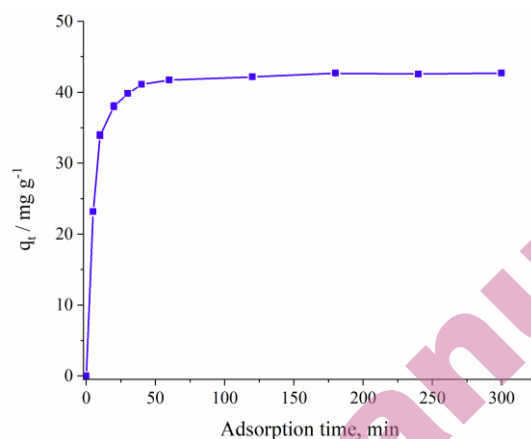


Fig. 3. MB adsorption kinetic onto pomegranate peel

TABLE II. Kinetic parameters for the adsorption of MB onto pomegranate peel

Kinetic model	Kinetic parameters at 298 K		Statistical analysis			
	$q_{e,cal} / \text{mg g}^{-1}$	K_1 / min^{-1}	R^2	RMSE	ARE%	χ^2
PFO	7.16	0.02	0.7857	34.43	88.75	$3.51 \cdot 10^3$
PSO	$q_{e,cal} / \text{mg g}^{-1}$	$K_2 / \text{g mg}^{-1} \text{min}^{-1}$	R^2	RMSE	ARE%	χ^2
	43.14	0.009	1	1.56	2.52	0.86
Elovich	$\alpha_E / \text{mg g}^{-1} \text{min}^{-1}$	$\beta_E / \text{g mg}^{-1}$	R^2	RMSE	ARE%	χ^2
	$2.11 \cdot 10^3$	0.26	0.7227	3.07	7.55	2.78
IPD (2)	$K_{ID} / \text{mg g}^{-1} \text{min}^{-1/2}$	c	R^2	RMSE	ARE%	χ^2
	1.13	33.41	0.9061	6.26	13.37	9.10

Furthermore, Fig. 4 (d) illustrates the tri-linearity observed in the IPD plot, which doesn't pass through the origin. This suggests that intraparticle diffusion is not the only rate-limiting step, and the MB adsorption process is controlled by three mechanisms. Indeed, the first linear section with a sharp slope represents the bulk diffusion at the adsorbent's external surface (instantaneous adsorption). The second section depicts intraparticle diffusion (gradual adsorption), and the last one, the plateau portion, represents equilibrium⁴⁴. The intercept of the second section provides information on the thickness of the boundary layer (Table II). A higher intercept indicates a thicker boundary layer, amplifying its effect^{45,46}. Other researchers have reported similar findings regarding the adsorption of MB onto tea residues and diatomite^{47,48}.

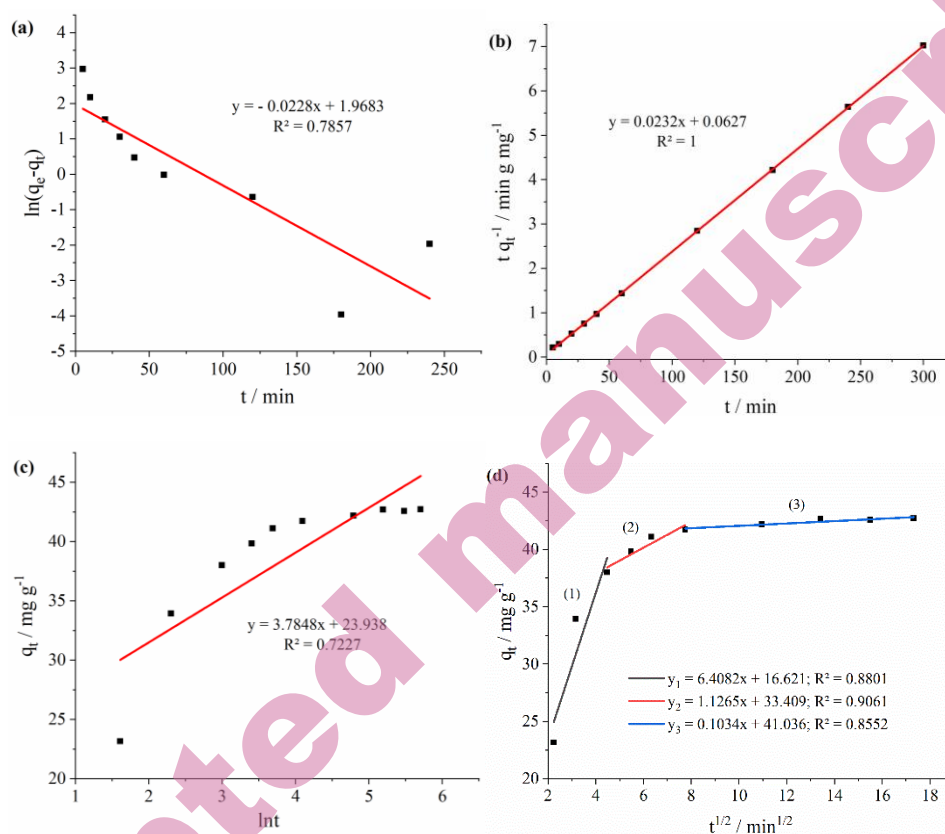


Fig. 4. PFO (a), PSO (b), Elovich (c), IPD (d) linear plots for MB adsorption onto pomegranate peel at 298 K

Models validation

Fig. 5 (a) depicts the accuracy of the PSO model in describing MB adsorption kinetic data. This observation is further supported by Fig. 5 (b), which provides a graphical comparison of the experimental and predicted equilibrium adsorption capacities for each model. The figure highlights the predictive quality of the PSO model in representing MB adsorption onto pomegranate peel, as evidenced by its closest predicted value ($q_{e,cal} = 42.76 \text{ mg g}^{-1}$) to the experimental value ($q_{e,exp} = 42.71 \text{ mg g}^{-1}$).

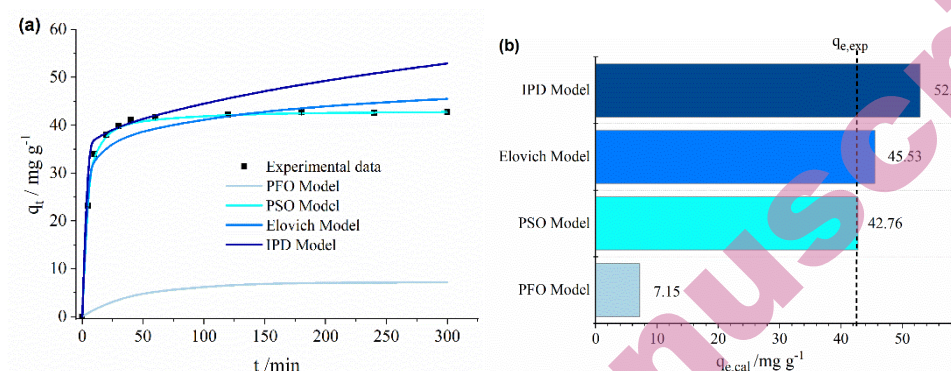


Fig. 5. Kinetic models validation with experimental data

Adsorption isotherm and modeling

The equilibrium mechanisms between MB and the pomegranate peel surface were studied through Langmuir and Freundlich models. The adsorption isotherm was simulated at 298 K (Fig. 6), and the associated parameters were determined and grouped with statistical analysis in Table III. The linear fitting plots of the Langmuir and Freundlich models are represented in Fig. 6. The Langmuir model provided a better fit to the experimental data, with a coefficient of determination closer to one ($R^2 = 0.9998$) and lower $RMSE$, ARE , and χ^2 values compared to the Freundlich model (Table III). This adequacy indicates monolayer adsorption of MB onto pomegranate peel.

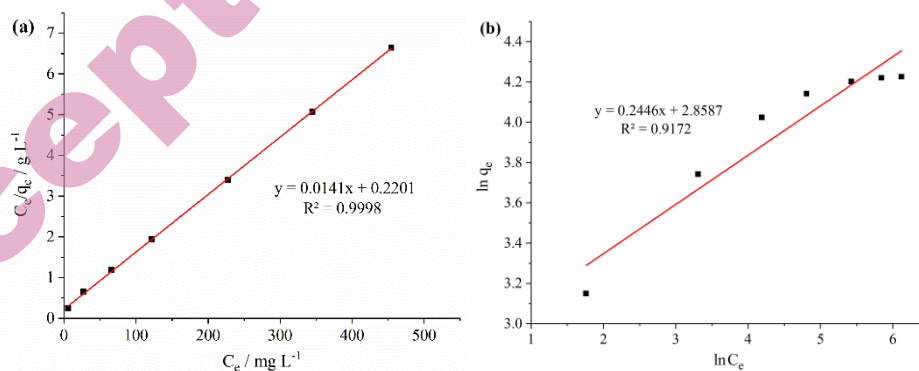


Fig. 6. Langmuir (a) and Freundlich (b) linear isotherm plots for MB adsorption onto pomegranate peel at 298 K

TABLE III. Equilibrium parameters for MB adsorption onto pomegranate peel at 298 K

Isotherm model	Isotherm parameters at 298 K		Statistical analysis			
	Langmuir	$q_{\max} / \text{mg g}^{-1}$	$KL / \text{L g}^{-1}$	R^2	RMSE	ARE %
	70.96	0.06	0.9998	2.00	4.05	1.10
Freundlich	n	$KF / (\text{mg g}^{-1})(\text{L g}^{-1})^n$	R^2	RMSE	ARE %	χ^2
	4.09	17.44	0.9172	5.72	9.69	4.01

The Langmuir model's adequacy is further supported by Fig. 7, which displays the experimental and predicted isotherms of MB adsorption onto pomegranate peel. A simple examination of the figure confirms the Langmuir model's predictive quality. Indeed, the Langmuir maximum adsorption capacity (70.96 mg g^{-1}) is close to the maximum experimental adsorption capacity (67.78 mg g^{-1}).

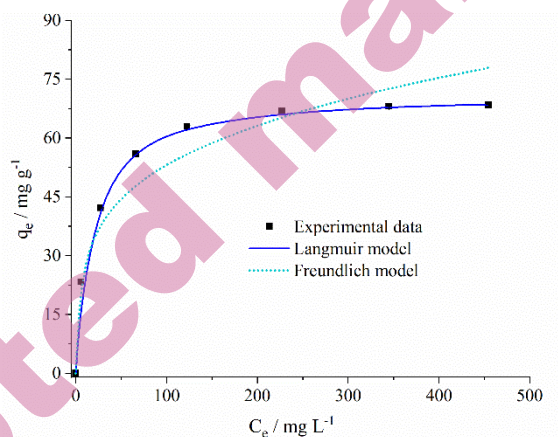


Fig. 7. MB adsorption isotherm onto pomegranate peel

Moreover, it is advisable to compare the adsorption capacity of pomegranate peel with that of other biomass reported in previous research. Table IV demonstrates that pomegranate peel has a higher adsorption capacity than other biomass, suggesting it could be used as an inexpensive and environmentally friendly adsorbent for removing MB.

TABLE IV. Comparison of maximum adsorption capacities of various biomass for MB dye

Biomass	$q_{\max} / \text{mg g}^{-1}$	Reference
Rice husk	40.59	4
Soursop residues	55.40	29
Sugarcane bagasse	17.43	29
Date pits	80.29	30
Wheat straw	60.66	32
Orange peel	18.60	33
Banana peel	20.80	33
Orange albedo	77.79	49
Potato peel	97.08	50
Avocado peel	62.11	51
Hamimelon peel	58.60	51
Dragon fruit peel	62.58	51
Tucuma cake	17.24	52
Pomelo peel	81.71	53
Pomegranate peel	67.78	This work

Thermodynamic study

The thermodynamic study plays an essential role in understanding the adsorption process of MB onto pomegranate peel. In this respect, thermodynamic parameters of MB adsorption, namely the free energy $\Delta G^\circ / \text{kJ mol}^{-1}$, the enthalpy $\Delta H^\circ / \text{kJ mol}^{-1}$, and the entropy $\Delta S^\circ / \text{J mol}^{-1} \cdot \text{K}^{-1}$ were determined using the following equations:

$$\Delta G^\circ = -RT \cdot \ln K_d; (K_d = \frac{q_e}{C_e}) \quad (8)$$

$$\Delta G^\circ = \Delta H^\circ - T\Delta S^\circ \quad (9)$$

$$\ln K_d = \left(\frac{\Delta S^\circ}{R} \right) - \left(\frac{\Delta H^\circ}{R} \right) \frac{1}{T} \quad (10)$$

where K_d is the distribution coefficient for adsorption, $C_e / \text{mg L}^{-1}$ is the equilibrium concentration of MB, $q_e / \text{mg g}^{-1}$ is the amount of MB adsorbed at equilibrium, T / K is the absolute temperature, and R is the gas constant ($8.314 \text{ J mol}^{-1} \text{ K}^{-1}$).

The slope and intercept of the $\ln K_d$ vs. T^{-1} plot, shown in Fig. 8, were used to calculate the values for ΔH° and ΔS° . Table V presents the derived results.

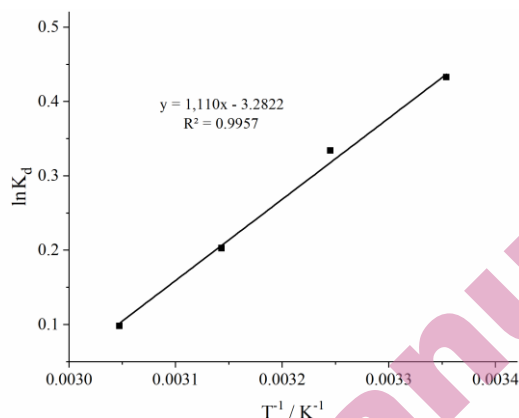


Fig. 8. The plot of $\ln K_d$ vs T^{-1} for the MB adsorption onto pomegranate peel

The negative values of ΔG° for the various temperatures examined, as shown in Table V, demonstrate the spontaneity of MB adsorption. The negative value of ΔH° supports the exothermic nature of the adsorption process and suggests the absence of energy required to transfer MB from the aqueous phase to the solid. Moreover, the negative value of ΔS° suggests a reduction in randomness at the adsorbent/adsorbate interface during the adsorption process without any significant change in the adsorbent structure⁵⁴. Similar findings were also reported by Miraboutalebi *et al.*⁵⁵ for the adsorption of MB onto corn silks.

TABLE V. Thermodynamic parameters

T / K	$\Delta G^\circ / kJ mol^{-1}$	$\Delta H^\circ / kJ mol^{-1}$	$\Delta S^\circ / J mol^{-1}K^{-1}$
298	-1.07	-9.23	-27.29
308	-0.86		
318	-0.54		
328	-0.27		

CONCLUSION

The findings indicate that pomegranate peel possesses a strong MB adsorption capacity. The MB adsorption occurred rapidly, reaching equilibrium around 60 minutes, with an adsorption capacity close to 42.71 mg g^{-1} at an initial dye concentration of 100 mg L^{-1} . The results from the kinetic approach suggest that MB adsorption onto pomegranate peel perfectly follows pseudo-second-order kinetic and that intraparticle diffusion is not the only rate-limiting step in the adsorption process. Additionally, a maximum adsorption capacity of 67.78 mg g^{-1} was observed with the isotherm approach, and equilibrium data showed good compliance with the Langmuir model. The exothermicity and spontaneity of the adsorption process were indicated by the negative values of ΔG° and ΔH° ,

respectively. In terms of ΔS° , the negative value suggested an increase in disorder at the adsorbent/adsorbate interface during the adsorption process. Moreover, pomegranate peel exhibited a comparatively higher adsorption capacity for MB compared to other biomass. These findings highlight the potential of pomegranate peel as an environmentally friendly adsorbent for effluent containing MB.

Acknowledgements: The authors acknowledge the CNRST (National Centre for Scientific and Technical Research, Morocco) for the partial support of this study.

ИЗВОД

ПЕРФОРМАНСЕ ЕКОЛОШКИ ПРИХВАТЉИВОГ АДСОРБЕНТА ЗА УКЛАЊАЊЕ МЕТИЛЕН ПЛAVОГ ИЗ ВОДЕНОГ РАСТВОРА: КИНЕТИЧКИ, ИЗОТЕРМНИ И ТЕРМОДИНАМИЧКИ ПРИСТУПИ

RAJAE GHIBATE¹, MERYEM BEN BAAZIZ², ALI AMECHROUQ³, RACHID TAOUIL⁴, OMAR SENHAJI³

¹Laboratory of Physical Chemistry, Materials and Environment, Faculty of Sciences and Technologies, Moulay Ismail University of Meknes, Errachidia, Morocco, ²Laboratory of Materials Engineering for the Environment and Natural Resources, Faculty of Sciences and Technologies, Moulay Ismail University of Meknes, Errachidia, Morocco, ³Laboratory of Biomolecular and Macromolecular Chemistry, Moulay Ismail University of Meknes, Meknes, Morocco, and ⁴Laboratory of Mechanics, Energetics, Automation, and Sustainable Development, Faculty of Science and Technology, Moulay Ismail University of Meknes, Errachidia, Morocco

Садашња студија има за циљ да утврди колико добро кора нара може уклонити метиленско плаво (МП) из воденог раствора. У ту сврху су спроведене кинетичке, изотермне и термодинамичке студије адсорпције у шаржном систему. Брзина адсорпције МП је била брза и достигла је равнотежу за око 60 минута. Достигнути капацитет адсорпције је близу 42,71 mg g⁻¹ при почетној концентрацији боје од 100 mg l⁻¹. Кинетичко моделирање адсорпције МП је спроведено коришћењем модела псеудо-првог, псеудо-другог реда, Еловича и модела дифузије унутар честица. Утврђено је да је модел псеудо-другог реда најадекватнији за уклањање кинетичких података на основу вредности R² (коэффициент детерминације), RMSE (квадратна средња грешка), ARE (просечна релативна грешка) и χ^2 (хи-квадрат). Такође је откривено да адсорпција МП на кори нара није једноставно ограничена брзином дифузије унутар честица. Изотермни приступ је показао максимални капацитет адсорпције од 67,78 mg l⁻¹ на 298 K коришћењем 2 g l⁻¹ коре нара. Такође је спроведено моделирање равнотеже. Четири статистичке вредности су истакле да се Лангмуров модел најбоље уклапа у односу на Фројндлихов модел. Додатно, егзотермна и спонтана природа процеса адсорпције је откривена термодинамичким истраживањем. Ови налази показују ефикасност коре нара као еколошки прихватљивог апсорбента за уклањање МП.

(Примљено 17. марта 2023; ревидирано 1. маја 2023; прихваћено 26. марта 2024.)

REFERENCES

1. Z. Y. Velkova, G. K. Kirova, M. S. Stoytcheva, V. Gochev, *J. Serb. Chem. Soc.* **83** (2018) 107–120 (<https://doi.org/10.2298/JSC170519093V>)

2. I. Khan, K. Saeed, I. Zekker, B. Zhang, A. H. Hendi, A. Ahmad, S. Ahmad, N. Zada, H. Ahmad, L. A. Shah, T. Shah, I. Khan, *Water* **14** (2022) 242 (<https://doi.org/10.3390/w14020242>)
3. H. Elmontassir, K. Elfalaki, Y. Karhat, M. Afdali, *Mor. J. Chem.* **7** (2019) 493–505 (<https://doi.org/10.48317/IMIST.PRSM/morjchem-v7i3.15882>)
4. V. Vadivelan, K. V. Kumar, *J. Colloid Interface Sci.* **286** (2005) 90–100 (<https://doi.org/10.1016/j.jcis.2005.01.007>)
5. T. K. Sen, S. Afroze, H. M. Ang, *Water. Air. Soil Pollut.* **218** (2011) 499–515 (<https://doi.org/10.1007/s11270-010-0663-y>)
6. M. W. Shannon, S. W. Borron, M. J. Burns, L. M. Haddad, J. F. Winchester, eds., *Haddad and Winchester's clinical management of poisoning and drug overdose*, 4th ed, Saunders/Elsevier, United States, 2007 (ISBN 10: 0721606938 ISBN 13: 978-0721606934)
7. Z. Cheng, R. Yang, X. Zhu, *Desalination Water Treat.* **57** (2016) 25207–25215 (<https://doi.org/10.1080/19443994.2016.1144535>)
8. H. Xue, X. Wang, Q. Xu, F. Dhaouadi, L. Sellaoui, M. K. Seliem, A. Ben Lamine, H. Belmabrouk, A. Bajahzar, A. Bonilla-Petriciolet, Z. Li, Q. Li, *Chem. Eng. J.* **430** (2022) 132801 (<https://doi.org/10.1016/j.cej.2021.132801>)
9. A. E. Badraoui, Y. Miyah, L. Nahali, F. Zerrouq, B. E. Khazzan, *Mor. J. Chem.* **7** (2019) 416–423 (<https://doi.org/10.48317/IMIST.PRSM/morjchem-v7i3.16742>)
10. N. Badri, Y. Chhiti, F. Bentiss, M. Bensitel, *Mor. J. Chem.* **6** (2018) 767–780 (<https://doi.org/10.48317/IMIST.PRSM/morjchem-v6i4.14350>)
11. A. Kesraoui, M. Seffen, F. Brouers, *Mor. J. Chem.* **5** (2017) 659–676 (<https://doi.org/10.48317/IMIST.PRSM/morjchem-v5i4.7250>)
12. S. Akazdam, W. Yassine, M. Chafi, B. Gourich, *Mor. J. Chem.* **7** (2019) 300–3013 (<https://doi.org/10.48317/IMIST.PRSM/morjchem-v7i2.14014>)
13. P. Colindres, H. Yee-Madeira, E. Reguera, *Desalination* **258** (2010) 154–158 (<https://doi.org/10.1016/j.desal.2010.03.021>)
14. A. H. Konsowa, *Desalination* **158** (2003) 233–240 ([https://doi.org/10.1016/S0011-9164\(03\)00458-2](https://doi.org/10.1016/S0011-9164(03)00458-2))
15. D. Wu, Z. Yang, W. Wang, G. Tian, S. Xu, A. Sims, *Chemosphere* **88** (2012) 1108–1113 (<https://doi.org/10.1016/j.chemosphere.2012.05.011>)
16. M. Ouhammou, M. Bouchdoug, A. Jaouad, R. Ouaabou, B. Nabil, *Mor. J. Chem.* **7** (2019) 516–527 (<https://doi.org/10.48317/IMIST.PRSM/morjchem-v7i3.16009>)
17. G. A. Ismail, H. Sakai, *Chemosphere* **291** (2022) 132906 (<https://doi.org/10.1016/j.chemosphere.2021.132906>)
18. Q. Li, Y. Li, X. Ma, Q. Du, K. Sui, D. Wang, C. Wang, H. Li, Y. Xia, *Chem. Eng. J.* **316** (2017) 623–630 (<https://doi.org/10.1016/j.cej.2017.01.098>)
19. J. Cheng, C. Zhan, J. Wu, Z. Cui, J. Si, Q. Wang, X. Peng, L.-S. Turng, *ACS Omega* **5** (2020) 5389–5400 (<https://doi.org/10.1021/acsomega.9b04425>)
20. Y.-Y. Lau, Y.-S. Wong, T.-T. Teng, N. Morad, M. Rafatullah, S.-A. Ong, *RSC Adv.* **5** (2015) 34206–34215 (<https://doi.org/10.1039/C5RA01346A>)
21. A. Othmani, A. Kesraoui, M. Seffen, *Euro-Mediterr. J. Environ. Integr.* **2** (2017) 1–12 (<https://doi.org/10.1007/s41207-017-0016-y>)
22. Q. Wei, F. O. Mcyotto, C. W. K. Chow, Z. Nadeem1, Z. Li, J. Liu, S. Desk, *J. Earth Sci. Environ. Stud.* **5** (2020) 51–60 (<http://dx.doi.org/10.25177/JESES.5.2.RA.10648>)

23. R. Ghibate, F. Sabry, O. Senhaji, R. Taouil, M. Touzani, *Int. J. Innov. Res. Sci. Technol.* **2** (2015) 39–48 (<http://www.ijirst.org/articles/IJIRSTV2I7003.pdf>)
24. L. Rozumová, O. Životský, J. Seidlerová, O. Motyka, I. Šafařík, M. Šafaříková, *J. Environ. Chem. Eng.* **4** (2016) 549–555 (<https://doi.org/10.1016/j.jece.2015.10.039>)
25. N. Karić, A. S. Maia, A. Teodorović, N. Atanasova, G. Langergraber, G. Crini, A. R. L. Ribeiro, M. Đolić, *Chem. Eng. J. Adv.* **9** (2022) 100239 (<https://doi.org/10.1016/j.cej.2021.100239>)
26. S. D. Abkenar, M. Hassannezhad, M. Hosseini, M. R. Ganjali, *J. Serb. Chem. Soc.* **84** (2019) 701–712 (<https://doi.org/10.2298/JSC181228038D>)
27. R. Ghibate, O. Senhaji, R. Taouil, *Case Stud. Chem. Environ. Eng.* **3** (2021) 100078 (<https://doi.org/10.1016/j.cscee.2020.100078>)
28. Q. Wang, Y. Wang, Z. Yang, W. Han, L. Yuan, L. Zhang, X. Huang, *Chem. Eng. J. Adv.* **11** (2022) 100295 (<https://doi.org/10.1016/j.cej.2022.100295>)
29. L. Meili, P. V. S. Lins, M. T. Costa, R. L. Almeida, A. K. S. Abud, J. I. Soletti, G. L. Dotto, E. H. Tanabe, L. Sellaoui, S. H. V. Carvalho, A. Erto, *Prog. Biophys. Mol. Biol.* **141** (2019) 60–71 (<https://doi.org/10.1016/j.pbiomolbio.2018.07.011>)
30. F. Banat, S. Al-Asheh, L. Al-Makhadmeh, *Process Biochem.* **39** (2003) 193–202 ([https://doi.org/10.1016/S0032-9592\(03\)00065-7](https://doi.org/10.1016/S0032-9592(03)00065-7))
31. R. Gong, M. Li, C. Yang, Y. Sun, J. Chen, *J. Hazard. Mater.* **121** (2005) 247–250 (<https://doi.org/10.1016/j.jhazmat.2005.01.029>)
32. Y. Wu, L. Zhang, C. Gao, J. Ma, X. Ma, R. Han, *J. Chem. Eng. Data* **54** (2009) 3229–3234 (<https://doi.org/10.1021/jc900220q>)
33. G. Annadurai, R. Juang, D. Lee, *J. Hazard. Mater.* **92** (2002) 263–274 ([https://doi.org/10.1016/S0304-3894\(02\)00017-1](https://doi.org/10.1016/S0304-3894(02)00017-1))
34. R. R. Mphahlele, P. B. Pathare, U. L. Opara, *Sci. Afr.* **5** (2019) 1–8 (<https://doi.org/10.1016/j.sciaf.2019.e00145>)
35. R. R. Ghibate, O. Senhaji, R. Taouil, *Int. J. Eng. Res. Appl.* **10** (2020) 19–22 (<http://www.ijera.com/papers/vol10no11/Series-1/C1011011922.pdf>)
36. I. Hmid, H. Hanine, D. Elothmani, A. Oukabli, *J. Saudi Soc. Agric. Sci.* **17** (2018) 302–309 (<https://doi.org/10.1016/j.jssas.2016.06.002>)
37. S. Azizian, *J. Colloid Interface Sci.* **276** (2004) 47–52 (<https://doi.org/10.1016/j.jcis.2004.03.048>)
38. Y. S. Ho, G. McKay, *Process Biochem.* **34** (1999) 451–465 ([https://doi.org/10.1016/S0032-9592\(98\)00112-5](https://doi.org/10.1016/S0032-9592(98)00112-5))
39. Y. S. Ho, G. McKay, *Process Saf. Environ. Prot.* **76** (1998) 332–340 (<https://doi.org/10.1205/095758298529696>)
40. M. Toor, B. Jin, *Chem. Eng. J.* **187** (2012) 79–88 (<https://doi.org/10.1016/j.cej.2012.01.089>)
41. I. Langmuir, *J. Am. Chem. Soc.* **38** (1916) 2221–2295 (<https://doi.org/10.1021/ja02268a002>)
42. A. H. Jawad, Y. S. Ngoh, K. A. Radzun, *J. Taibah Univ. Sci.* **12** (2018) 371–381 (<https://doi.org/10.1080/16583655.2018.1476206>)
43. H. Li, V. L. Budarin, J. H. Clark, M. North, X. Wu, *J. Hazard. Mater.* **436** (2022) 129174 (<https://doi.org/10.1016/j.jhazmat.2022.129174>)
44. N. S. Randhawa, N. N. Das, R. K. Jana, *Desalination Water Treat.* **52** (2014) 4197–4211 (<https://doi.org/10.1080/19443994.2013.801324>)
45. F.-C. Wu, R.-L. Tseng, R.-S. Juang, *Chem. Eng. J.* **153** (2009) 1–8 (<https://doi.org/10.1016/j.cej.2009.04.042>)

46. G. Crini, E. Lichtfouse, *Green adsorbents for pollutant removal : fundamentals and design*, Springer, Germany, 2018 (<https://doi.org/10.1007/978-3-319-92111-2>)
47. N. Nasuha, B. H. Hameed, A. T. M. Din, *J. Hazard. Mater.* **175** (2010) 126–132 (<https://doi.org/10.1016/j.jhazmat.2009.09.138>)
48. M. A. Al-Ghouti, M. A. M. Khraisheh, M. N. M. Ahmad, S. Allen, *J. Hazard. Mater.* **165** (2009) 589–598 (<https://doi.org/10.1016/j.jhazmat.2008.10.018>)
49. C. E. de F. Silva, B. M. V. da Gama, A. H. da S. Gonçalves, J. A. Medeiros, A. K. de S. Abud, *J. King Saud Univ. Eng. Sci.* **32** (2020) 351–359 (<https://doi.org/10.1016/j.jksues.2019.04.006>)
50. K. Ben Jeddou, F. Bouaziz, F. Ben Taheur, O. Nouri-Ellouz, R. Ellouz-Ghorbel, S. Ellouz-Chaabouni, *Water Sci. Technol.* **83** (2021) 1384–1398 (<https://doi.org/10.2166/wst.2021.075>)
51. R. Mallampati, L. Xuanjun, A. Adin, S. Valiyaveetil, *ACS Sustainable Chem. Eng.* **3** (2015) 1117–1124 (<https://doi.org/10.1021/acssuschemeng.5b00207>)
52. Z. M. Magriotis, S. S. Vieira, A. A. Saczk, N. A. V. Santos, N. R. Stradiotto, *J. Environ. Chem. Eng.* **2** (2014) 2199–2210 (<https://doi.org/10.1016/j.jece.2014.09.012>)
53. Y. Ren, C. Cui, P. Wang, *Molecules* **23** (2018) 1342 (<https://doi.org/10.3390/molecules23061342>)
54. L. A. da Silva, S. M. S. Borges, P. N. Paulino, M. A. Fraga, S. T. de Oliva, S. G. Marchetti, M. do C. Rangel, *Catal. Today.* **289** (2017) 237–248 (<https://doi.org/10.1016/j.cattod.2016.11.036>)
55. S. M. Miraboutalebi, S. K. Nikouzad, M. Peydayesh, N. Allahgholi, L. Vafajoo, G. McKay, *Process Saf. Environ. Prot.* **106** (2017) 191–202 (<https://doi.org/10.1016/j.psep.2017.01.010>).